UDK 662.2.036:621.771.8:669.715
Original scientific article/Izvirni znanstveni članek

ISSN 1580-2949
MTAEC9, 50(6)861(2016)

ANALYSIS OF TWIN-ROLL CASTING AA8079 ALLOY 6.35-μm FOIL ROLLING PROCESS

ANALIZA PROCESA VALJANJA 6,35 μm FOLIJE IZ ZLITINE AA8079 ULITE MED DVEMA VALJEMA

Ahmet Can[1], Hüseyin Arikan[2], Kadir Çınar[2]

[1]Necmettin Erbakan University, Faculty of Engineering, Department of Industrial Design, Konya, Turkey
[2]Necmettin Erbakan University, Faculty of Engineering, Department of Mechanical Engineering, Seydişehir, Konya, Turkey
ahmetcan@konya.edu.tr

Prejem rokopisa – received: 2015-06-29; sprejem za objavo – accepted for publication: 2015-12-16

doi:10.17222/mit.2015.134

In this work the rolling process and properties of a 6.35-μm twin-roll casting AA8079 aluminum alloy foil was analyzed. First, the 8-mm-thick sheets were produced with a twin-roll casting technology. This product was annealed and cold rolled to a 6.35-μm foil with suitable processing conditions. The mechanical tests and microhardness measurement was applied to specimens derived from all the foil-rolling process stages. On the other hand, the specimens' surface roughness and the surface structure are visualized with an atomic force microscope and an SEM. The microstructural investigation is realized with an optical microscope and XRD. The von-Misses total effective strain was calculated by determining the incremental work for all of the cold-rolling cycle. The alloy showed very low ductility in the tensile tests because of the second-phase metastable intermetallic particles such as Al_3Fe. The maximum elongation at the breaking value was measured for 256-μm-foil as 4.5 %. On the other hand, the alloy did not show any significant strain hardening after the cold rolling during the plastic-deformation stages.

Keywords: aluminum foil, cold rolling, twin roll casting

V delu je bil analiziran postopek valjanja in latnosti 6,35 folije iz AA8079 aluminijeve zlitine, ulite med dvema valjema. Najprej je bil izdelan 8 mm debel trak po postopku ulivanja med dvema valjema. Trak je bil primerno žarjen in hladno zvaljan v 6.35 μm folijo. Iz vseh stopenj procesa valjanja so bili vzeti vzorci na katerih so bile določene mehanske lastnosti in izmerjena mikro trdota. Poleg tega je bila hrapavost površine in struktura površine vizualizirana z mikroskopom na atomsko silo (AFM) in iz SEM. Preiskava mikrostrukture je bila izvršena s svetlobnim mikroskopom in z rentgensko difrakcijo (XRD). Za določanje stopnjujočega dela, med celotnim ciklom hladnega valjanja, je bila izračunana celotna von-Misses efektivna napetost. Zlitina je pokazala zelo nizko duktilnost pri nateznih preizkusih zaradi vsebnosti delcev sekundarne metastabilne intermetalne faze Al_3Fe. Maksimalni raztezek pri porušitvi je bil pri 256 μm debeli foliji 4.5 %. Po drugi plati pa zlitina ni kazala nobenega občutnega napetostnega utrjevanja med posameznimi fazami plastične deformacije.

Ključne besede: aluminijeva folija, hladno valjanje, ulivanje med dvema valjema

1 INTRODUCTION

The production of aluminum alloys with twin roll casting (TRC) technology has been introduced to the industry about 50 years ago. It was claimed that TRC would offer significant reduction in the cost of aluminum sheet and foil production, compared to the conventional production technique, i.e. DC casting and hot rolling. Major evolution in the TRC technology has been attained in the last 5 years. It has been widely accepted due to its low investment cost, operational cost and flexibility provided to the production planning.[1]

The strengthening of metals due to increase in lattice defects during cold deformation makes a thermodynamically unstable structure and promotes subsequent restoration phenomena. The restoration processes can change microstructures as well as mechanical and physical properties of metals and alloys while required mechanical and physical properties may be achieved by adjusting the deformation and annealing variables.[2] Some of the researchers[3–6] studied about cold rolling of various aluminum alloys. D. Wang et al.[3] studied about severe cold rolling (CR) deformation properties of AA 7050. The strength of the 7050 samples increased with increasing the CR reduction. The yield and ultimate strengths of the CR sample with a reduction of 67 % increased by 16.5 % and 9.2 %, respectively. Wang reported that both the residual dislocations and heterogeneously nucleated fine-phase particles in the matrix increased the strength of the CR samples.

Z. Liang et al.[4] studied the evolution of texture as well as microstructures in an AA 7055 aluminum alloy during cold rolling. Author reported that more micro-bands are formed in the center of the plate with the rolling reduction, while the spacing between two bands decreases.

S. X. Zhou et al.[5] studied about cold Rolling of AA 1050 alloys which are produced by hot finishing rolling and twin roll casting. Authors studied the microstructure mechanical properties such as tensile strength, yield stress elongation area reduction, elastic modulus hardness and impact energy and formability.

J. G. Lenard[6] studied the effect of roll roughness on the rolling parameters during cold rolling of 6061-T6 alloys. The effects of the roughness of the work roll on the roll force roll torque and the forward slip and additionally the frictional mechanisms were identified. Author reported that high roughness appeared to increase the possibility of insufficient lubrication at the interfaces. While both adhesive and ploughing forces were present in all instances, the ploughing forces became dominant at higher rolling speeds. The contribution of ploughing to frictional resistance increased as the roll roughness increased to a certain value and beyond that its behavior depended on the rolling speed. J. G. Lenard and S. Zhang[7] studied a similar work with commercially pure aluminum. Using lighter oil, boundary or mixed lubrication is produced. With higher viscosity oil, negative forward slip is observed, indicating the onset of hydrodynamic lubrication. The coefficients of friction are found to increase with increasing reduction and decreasing rolling speeds.[7]

K. S. S. Sathees et al.[8] studied about with purity aluminum sheets which were subjected to intense plastic straining by constrained Groove pressing method. The tensile behavior evolution with increased straining indicates substantial improvement of yield strength by 5.3 times from 17 MPa to 90 MPa during first pass corroborated to grain refinement observed. Quantitative assessment of degree of deformation homogeneity using micro hardness profiles reveal relatively better strain homogeneity at higher number of passes.

G. Liv[9] studied the development of surface structure forming properties and corrosion resistance during cold rolling of twin-roll cast of AA 3003. It is found that the as-cast surface determines the development of the surface topography during cold rolling. This is due to the large roughness associated with the groove/shingle configuration of the as-cast surface. Author pointed out that, the initial surface topography and the cold rolling are of great importance to the quality of the end product of the cold rolling. Since there are differences in the initial topography induced by the surface of the casting rolls, there will be differences in the development of the surface during the deformation sequence. The rough pattern of the as-cast surface results in large gorges in the first pass. In the second pass shingles are smeared out on top of the gorges. Patches of the shingle are not welded to the bulk sheet.

It must be focused to metallurgical principles of Aluminum alloys for determining the mechanical and formability behavior of Al-Fe alloys. The main concern is propagation of second phase intermetallic particles which is a function of both the cooling rate and the chemical composition of Al–Fe alloys and their effects on mechanical properties. Some of the researchers focused the metallurgical behavior of Al-Fe powders and alloys.[10–13] On the other hand some of the researchers focused the rapid cooling rate and severe deformation effects on the different Al-Fe alloys.[14–16] M. Aghaie-Khafri and R. Mahmudi[17] have investigated the plastic instability and necking behavior of AA8079 aluminum alloy sheet in temper-annealed and fully annealed conditions.

In this work, the rolling process and properties of 6.35 mm twin roll casting AA8079 aluminum alloy foil was analyzed. Foils production were tested on the level of industrial trials with no rupture by the time rolling process. Firstly the 8 mm thickness sheets were produced by twin roll casting technology. This product was annealed and cold rolled to 6.35 μm foil with suitable process conditions. The mechanical tests and micro hardness measurement is applied to specimens derived from whole foil rolling process stages. On the other hand the specimens' surface roughness and the surface structure is visualized with Atomic Force Microscope and SEM.

2 MATERIAL AND EXPERIMENTAL PART

The material used in this experimental investigation was an aluminum-rich eutectic alloy AA8079. As derived from XRF analyses the alloy containing (in mass fractions, w/%) 99 % Al, 0.8 % Fe and 0.12 % Si with minor constituents of 0.02 % Cu, 0.02 % Mn, 0.009 % Zn, and 0.022 % Ti. Notice that this work is not only an experimental work. The whole experimental outputs were derived from a real industrial production process. So, nearly 2000 kg raw material of AA8079 was melted and roll-casted to 8 mm thickness and cold rolled to 4 mm at one step in CR (Cold Rolling Machine). Then the material homogenized at 580 °C for 8 h, furnace cooled, and then cold rolled to the thickness 0.53 mm with four steps. Then the material annealed in a furnace at 450 °C and a holding time of 4 h. Then cold rolled to the initial foil thickness 250 μm with one step. The 250 μm sheet was cold rolled to 100 and then 56 μm with two steps in FR-I rolling machine. The 56 μm foil was cold rolled to 14 μm with two steps in FR-II rolling machine. Then the final thickness foil was derived by cold rolling with twofold (14+14 μm foil on foil) foil in FR-III rolling machine. The diameter of the (CR) cold rolling pin was 400 mm, and the foil rolling (FRI-III)) pin was 240 mm. The Rolling speed of CR, FRI,FRII,FRIII were, 12-175-325-560 m/min respectively. After final (6.35 μm) cold rolling, the annealing in a furnace at 270 °C and a holding time of 11 h is applied.

The experimental samples were derived from all rolling stages. All the experimental numeric outputs such as tensile-yield strength, elongation at break and surface roughness values verified with minimum 3 times repeated tests results. These outputs were averaged and given with derived error band in the graphs. The micro hardness test was realized in NDT MH-140 under 5 g loading forces. The surface roughnesses of the foils were measured with Mitutoyo Surf Test SJ301 roughness measurement device. The 3D surface topography was determined with Park XE-100 Atomic Force Microscope

(AFM). The samples were polished with Struers polishing devices with suitable abrasives. The specimens thinner than 250 μm etched with 0.5 % HF solutions in 30 s and then cleaned with alcohol and dried with air. 8-4-2 mm specimens were etched electroliticaly under the 24 °C, 18 V electric current in a 5 % Tetra Fluoroboric acid solution in 120 s. And Nikon stereo light microscope is used for determining the microstructure with X10-500 magnification. The grain dimensions are derived with ASTM E112. The tensile tests were realized with Testometrik DBBMTCL-250 Kgf device. And the pinhole counting is realized with special lighting table with BS-EN 546-4 procedures.

3 RESULTS AND DISCUSSION

3.1 Mechanical properties

A tensile test procedure is applied after all foil cold rolling stages and annealing procedures. The ultimate engineering stress before rupture of specimen, Engineering Tensile Stress (σ_u), Yield Stress ($\sigma_{0.2}$) and Strain at Failure (ε_f) values were determined with 100 mm initial length samples (A_{100}). Nearly same tendency and graphics were observed in all tensile tests for cold rolled specimens. A specific stress-strain graphics for AA8079 were given in **Figure 1** as representative. Aluminum on the other hand having a FCC crystal structure does not show the definite yield point in comparison to those of the BCC structure materials, but shows a smooth engineering stress-strain curve. The yield strength ($\sigma_{0.2}$) therefore has to be calculated from the load at 0.2 % strain. It can be observed from **Figure 1** that the material does not show any significant strain hardening after yield point. It causes the develop plastic instability and, thereby, very low ductilities. When this situation compared with the previous researchs the same tendency is observed. This undesirable phenomenon and the associated strain localization can be avoided by employing annealing process.[17]

The von-misses total effective strain (ε_{vm}) was calculated for determining the incremental work for all cold rolling cycle. **Figure 2a** shows the ε_{vm} versus (Tensile Stress) σ_u, **Figure 2b** shows the ε_{vm} versus (Yield Stress) $\sigma_{0.2}$. As can be seen in **Figures 2a** and **2b** an increase can be observed in after first cold Rolling (ε_{vm} = 1.5). It can be explained by strain hardening of cold worked alloy. But nearly no change was observed on tensile and the yield stress between ε_{vm}= 1.5 and 4.2. It can be explained by very low and saturated strain hardening and very long post uniform elongations as depicted in stress-strain curve in **Figure 1**. Notice that the AA8079 material includes 99 % pure aluminum. When the tensile and yield strength graphs are compared with the previous researcher result the same tendency can be observed. K. S. S. Satheesh and T. Raghu[8] reported that the yield strength ($\sigma_{0.2}$) increases significantly after first pass of cold working, whereas the tensile strength (σ_u) is nearly showed same behavior. Considerable increase in strength observed after first pass is mainly attributed to the significant decrease in

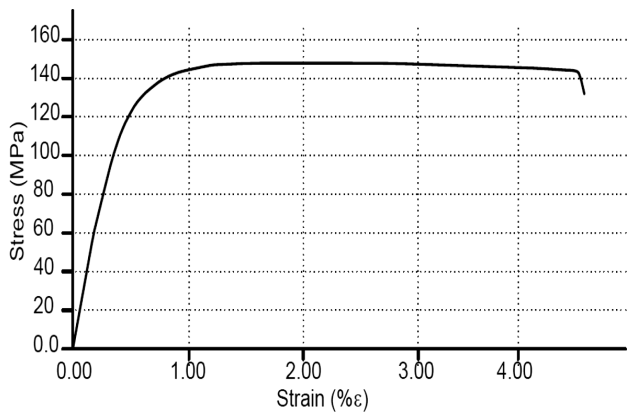

Figure 1: The stress-strain graphic for 256 μm specimen
Slika 1: Diagram napetost-raztezek za vzorec debeline 256 μm

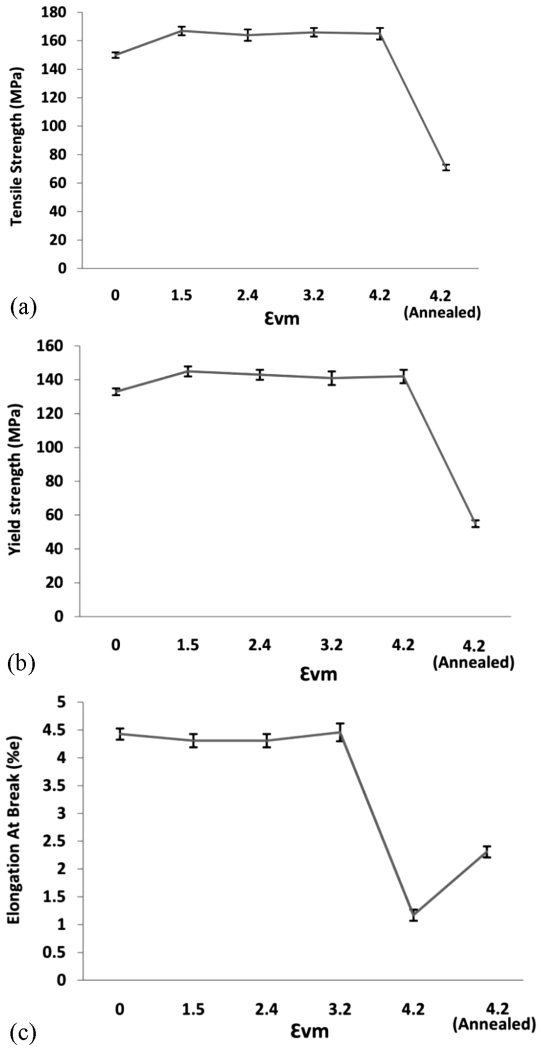

Figure 2: The effect of equal strain on mechanical properties: a) tensile strength, b) yield strength, c) elongation at break
Slika 2: Vpliv enake napetosti na mehanske lastnosti: a) natezna trdnost, b) meja plastičnosti, c) raztezek ob porušitvi

grain sizes and the increased dislocation density which necessitates higher applied stress for dislocation motion by slip. A horizontal trend in $\sigma_{0.2}$ & σ_u is observed in subsequent passes which is attributed to the increased recovery/annihilation of dislocations with increasing accumulated strain and formation of micro cracks. Propagation of intermetallic phases in structure has great affect on mechanical properties. Previous researchers indicate that the intermetallic phases reduce the strength and elongation capability of the aluminum alloys. When tensile fracture surfaces of aluminum alloy samples investigated with SEM, it is observed that fracture occurs secondary intermetallic phases and inclusion concentration regions.[18]

P. J. Appsa et al.[15] investigated the effect of coarse second-phase particles on the rate of grain refinement and material properties during severe deformation processing. Authors indicate that the hardness development of the AA8079, with increasing deformation process strain and the hardness of the AA8079 was slightly higher than that of the single-phase alloy, due to the presence of the second-phase particles. During deformation, the work hardening of the AA8079 alloy saturated much more rapidly than the single-phase alloy and reached a plateau at a strain of only ε_{vm}~3 showing little further increase even after a strain of 10. This behavior would be expected to correspond to a continued fast micro structural refinement with increasing strain.

The restoration processes can change microstructures as well as mechanical and physical properties of metals and alloys while required mechanical and physical properties may be achieved by adjusting the deformation and annealing variables.[2] The annealing process was decreased the tensile and the yield strength significantly. Reversely the annealing process was increased the elongation at break values. The maximum elongation at break ε_f value is observed as 4.4 from 250 μm to 15 μm foils. This value was decreased to 1.2 % for final 6.5 μm foils. Then the last foil annealing treatment increased the elongation value to 2.3 %. It can be concluded that the recovery phenomenon is the major reason of decrease in flow stress. The steep increase in ductility implies that a complete softening due to recrystallization and grain refinement has taken place, and there covered structure, which is expected to be the main cause of the observed premature failure, has been removed.[8,17]

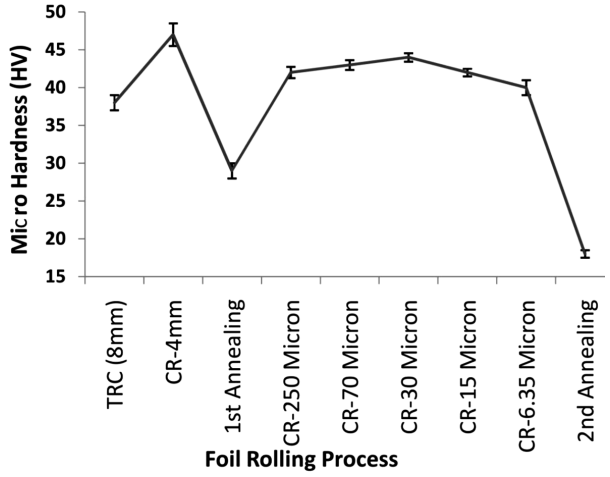

Figure 3: The variation of Micro hardness of the foils during cold rolling
Slika 3: Spreminjanje mikrotrdote folij med hladnim valjanjem

Figure 3 shows the micro-hardness results of the rolling stages from TRC to last foil annealing. The first cold rolling process after TRC is decreased to micro-hardness from 38 HV to 47 HV. During the deformation process, after the 1st annealing process the hardness of the alloy saturated rapidly and reached a plateau at a 250 μm thickness. This behavior would be expected to correspond to a continued fast micro structural refinement with increasing strain. The annealing at 450 °C and a holding time of four hours decreased the micro-hardness from 47 HV to 29 HV. After annealing the cold rolling was decreased to 29 HV to 42 HV and the micro hardness has no significant change during the cold rolling process until the last annealing process. The micro hardness was decreased to the least value after the last foil annealing process. As compared the micro hardness behavior with previous works; the results are coinciding with each other. Salehi reported the variation of micro-hardness after cold rolling with 20 %, 30 % and 40 % reduction in thickness. As a result, increased cold working increases the micro-hardness of the structure by increased dislocation density and deformed grains.[2,8,15] There is significant increase in hardness after first pass, after 1st annealing followed by marginal increase after second pass. During subsequent passes the hardness drops slightly and tends to remain fairly uniform fairly coinciding with earlier findings.[8]

After final cold rolling 14 μm to 6.5 μm, (ε_{vm} =4.2) the annealing in a furnace at 270 °C and a holding time of 11 h is applied. This treatment reduced the tensile and the yield strength of the materials 71 MPa and 55 MPa respectively. The cold rolled and annealed 6.5 μm foils stress-strain graphics were depicted in **Figures 4a** and **4b**.The cold rolled 6.5 μm foil has showed maximum elongation ε = 1.2. This value was increased to 2.3 % after the last annealing process. These elongations at break values show that this material can be called a brittle material because of low ductility. This undesirable phenomenon and the associated strain localization can be avoided by employing suitable annealing procedures. The annealed specimen's tensile graphics has some differences from cold rolled specimens. The annealed specimens showed a dynamic deformation aging behavior or The Portevin–Le Chatelier effect (PLC) effect. PLC describes a serrated stress-strain curve or jerky flow, which some materials exhibit as they undergo plastic deformation. This behavior is an expected behavior on annealed aluminum alloys only in limited regimes of strain rate. In a uniaxial tension test for instance, this

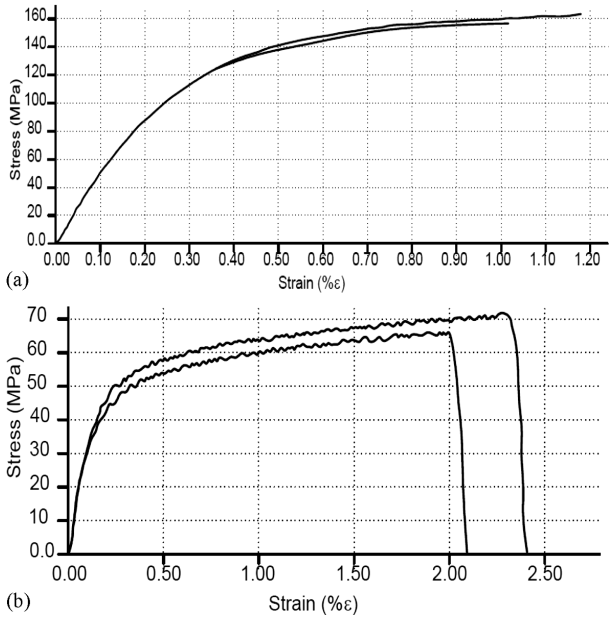

Figure 4: The stress-strain graphic for 6.5 μm specimen: a) cold rolled, b) annealed-270 °C, 11 h

Slika 4: Diagrami napetost-raztezek pri vzorcu debeline 6,5 μm: a) hladno valjano, b) žarjeno 270 °C, 11 h

irregular flow results in inhomogeneous deformation with various localization bands. These bands can be static, hopping and sometimes propagating along the specimen. It is also observed in presence of this irregular flow that some materials fail by a shear localization mode prior to any diffuse necking in uniaxial tension and even under more complex states of stress.[19]

3.2 Microstructure properties

The samples were characterized by XRD with a Bruker D8 advance diffractometer (40 kV, 40 mA), in Bragg-Brentano reflection geometry with Cu-$K\alpha$ radiation (λ = 0.154 nm). The data were obtained between 10° and 90° in steps of 0.1 with counting time of 3.

When the previous research are investigated various author focused the intermetallic phase formation. On the other hand some of the researchers focused the TRC process which is very important the on the effect on cooling rate. Al-rich portion of the Al–Fe binary phase diagram shows many intermetallic formed by the peritectic reactions.[13] The $Al_{13}Fe_4$, Al_5Fe_2, Al_3Fe (Al_nFe_m) etc. are possible intermetallic phases in Aluminum alloys.[1,10] **Figure 5** shows the XRD diffractogram pattern of the 6.35 μm foil of AA8079 alloy. The peak in 2θ 78° indicates the α-Al (311) with miller index. The remaining peaks indicate Al_3Fe intermetallic phases. Alloying of Al with Fe increases the high temperature strength due to a dispersion of second phase particles. Some of the researchers[15] introduces this Al_3Fe intermetallic peak as $Al_{13}Fe_4$. On the other hand some of the researcher reported that, these two monoclinic structural submicron intermetallics are very close to each other.[12,20]

The rapid cooling and solidification have great effect on formation of the intermetallic phase. However, the development of solidification microstructures along the (Twin Roll Casting) TRC process has some particular characteristics. The TRC makes the solidification with water cooled cylinders and it causes high cooling rate solidification and deforming near the surface.[1] High cooling rates near the surface cause the formation of metastable intermetallic Al_6Fe and Al_mFe compounds in addition to the stable Al_3Fe. It is often considered that at high cooling rates, due to kinetic restrictions there is not enough time for the atoms to arrange themselves in a stable structure.[1,13] During the cooling stage no nucleation is involved and an epitaxial solidification occurs. Moreover, the onset of solidification at the molten substrate interface is characterized by a solidification velocity that approaches zero, favoring the initial formation of the stable Al–Al_3Fe eutectic. This structure probably continues to grow in spite of the sudden increase in the solidification velocity over the surface, i.e., the equilibrium Fe aluminide is not displaced with increasing solidification velocity by a metastable aluminide.[10,14,15]

Previous researchers reported that the Si content is lower than 0.15 % of mass fractions of Si, which is the limiting Si content permitting to avoid AlFeSi to be the dominant intermetallic phase.[16] The material used in the experiment (AA8079) has the Si ratio of 0.12 and no AlFeSi intermetallic was observed in the structure.

A microstructure samples were derived after all rolling process. The procedure for etching and electro polishing for thick specimens was described in the previous sections. **Figures 6a** and **6b** shows the etched and electro polished optical microscope images respectively. As depicted in **Figures 6a** and **6b** the intermetallic phases needles oriented along the nonhomogeneous grains. Orientation along the casting directions between the grains boundaries were not observed on 8 mm TRC samples. The 8 to 4 mm cold rolled specimen's microstructure was depicted in **Figures 6c** and **6d**. The effect

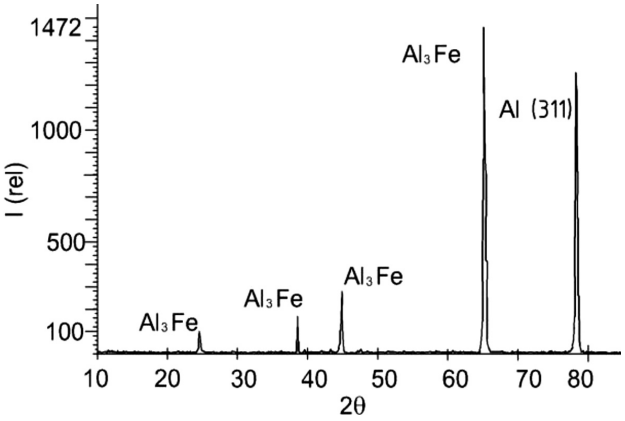

Figure 5: X-ray diffractogram of the Twin Roll Casting 6.35 μm AA8079 Foil

Slika 5: Rentgenogram 6,35 μm folije iz traku AA8079, ulitega med dvema valjema

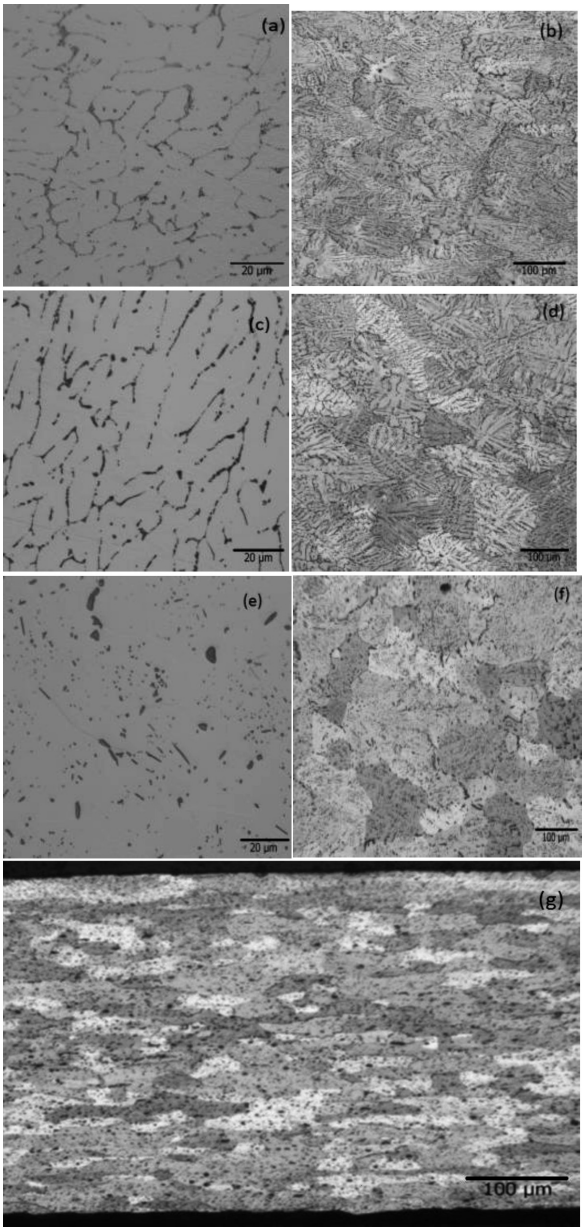

Figure 6: Etched and electro polished light microscope images: a), b) twin roll casting, c), d) cold rolled, e), f) 580 °C, 8 h annealed and g) 250 μm foil rolling samples

Slika 6: Mikrostruktura po jedkanju in elektropoliranju: a), b) ulito med dvema valjema, c), d) hladno valjano, e), f) žarjeno 8 ur na 580 °C in g) vzorec valjane 250 μm folije

of the 50 % plastic deformation on cold rolling can be observed on these figures. The narrowing affect along the grain boundary can be observed as comparing the **Figures 6a** and **6c**. After 4 mm cold rolling process the annealing (580 °CC – 8 h) is applied before the foil rolling process. **Figures 6e** and **6f** show the annealed samples microstructure. The needle shape of the intermetallic particles transforms to bulk shape by the recovery effect. The microstructures of the 250 μm to 6.5 μm foil specimens' light microscope images were determined. The 250 μm foil microstructure is depicted in **Figure 6g** as representative. As depicted in **Figure 6g** the grains are

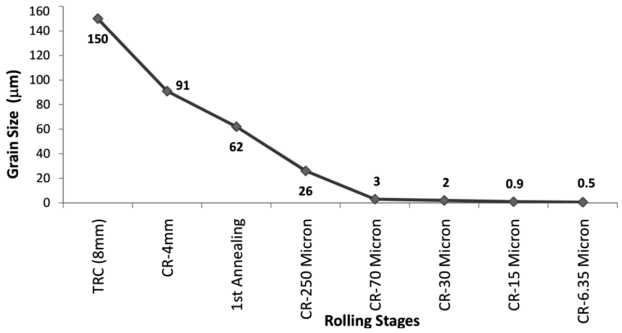

Figure 7: The variation of grain size with TRC to foil rolling stages

Slika 7: Spreminjanje velikosti zrn od TRC do končne izvaljane folije

elongated along the rolling direction and the narrowed vertically to rolling direction by comparing the previous stage microstructure as given in **Figures 6a** and **6f**.

The distance between intermetallic particles are decreased with increased plastic deformation ratio. The grain size vertically to rolling direction is measured with image processing and illustrated with grain size vs rolling stages from TRC to 6.5 μm foil in **Figure 7**. As depicted in **Figure 7** the grain size was decreased from 150 μm to 0.5 μm. After $\varepsilon_{vm} = 2.4$ strain, the submicron grain size were observed in the microstructure.

3.3 Surface properties

Not only the metallurgical and mechanical properties of the aluminum sheets and foils are very important, but also the surface properties of the aluminum sheets and foils are very important and it must be characterized to

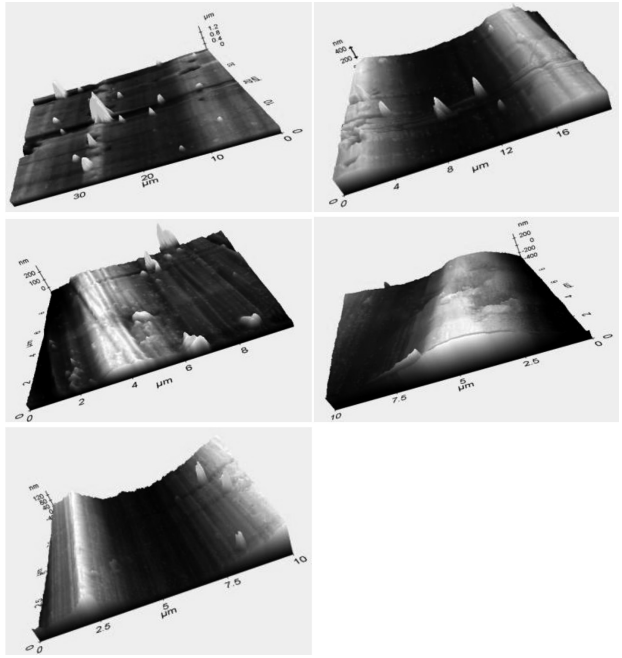

Figure 8: The atomic force microscope visualization of the thin foils from 250 to 6.5 μm

Slika 8: Vizualizacija površine folij od 250 μm do 6,5 μm, z mikroskopom na atomsko silo

desired functions as where they used. The chemical and electrochemical surface properties and the surface structure are very important in lithography sheets and also in food industry. In contrary to hydrophilic lithography sheets the surface must be smooth and shiny in food industry. So in this work the surface properties were determined with atomic force microscope (AFM), surface roughness measurement and optical microscope. And also the pin holes and rolling tracks were determined with the SEM and optically with light source. The AFM scanning images were depicted in **Figure 8** from 250 μm to 6.5 μm. Notice that the vertical scale is used as μm and nm depending on the roughness of the samples. The valley and the peaks are oriented along the rolling direction. **Figure 9** shows the surface roughness of the rolled samples and the roller pins surface roughness. As depicted in **Figure 9** the surface roughness is decreased with rolling stages. The surface roughness of the rolling pin and the foils are very close in almost all cases especially in thinner foils.

The pin hole counting is realized with a special light source in an dark ambient. The holes are counted for per 1 dm^2 as detailed in ISO-EN 546-4. **Figure 10a** shows a sample pin hole SEM images. The pin hole diameter is measured as 1 μm and meanly 10 pin holes are counted in 1 dm^2 standard area. And also the rolling tracks, porous and the skid effected banked up structure can be observed from **Figures 10a** and **10b**.

4 CONCLUSION

Foils production were tested on the level of industrial trials with no rupture by the time rolling process. It has been shown that selected TRC parameters result in the production of 8 mm sheet of good quality, with especially: fine microstructure with adequate grain refiner addition and annealing conditions.

Although the hard phases (that could lead to porosity problems) in the microstructure the 8 mm to 6.35 μm foil rolling was realized by obtaining the adequate surface properties such as sufficient pin hole, porosity

The von-misses total effective strain was calculated for determining the incremental work for all cold rolling cycle. After first cold rolling (ε_{vm} = 1,5) the yield and the tensile stress were increased in a limited range. This increase was explained by strain hardening of cold worked alloy. After continued deformation no change was observed on tensile and the yield stress between ε_{vm} = 1.5 and 4.2. It can be explained by nearly saturated strain hardening behavior after a critical plastic deformation.

On the other hand the maximum elongation at break ε_f value is observed as 4.4 from 250 μm to 15 μm foils. These elongations at break values show that this material can be called a brittle material because of low ductility.

The first cold rolling 8 mm to 4 mm process after TRC is decreased to micro hardness to the highest value of 47 HV. During the deformation process, after the 1st annealing process the hardness of the alloy saturated rapidly and reached a plateau at a 250 μm thickness. This behavior would be expected to correspond to a continued fast microstructure refinement with increasing strain.

The annealed foil specimens showed a dynamic deformation aging behavior or The Portevin–Le Chatelier effect (PLC) effect in tensile test. PLC describes a serrated stress-strain curve or jerky flow, which some materials exhibit as they undergo plastic deformation.

The XRD analyses shows that the TRC casting AA8079 alloys includes α-Al (311) and the Al_3Fe meta-

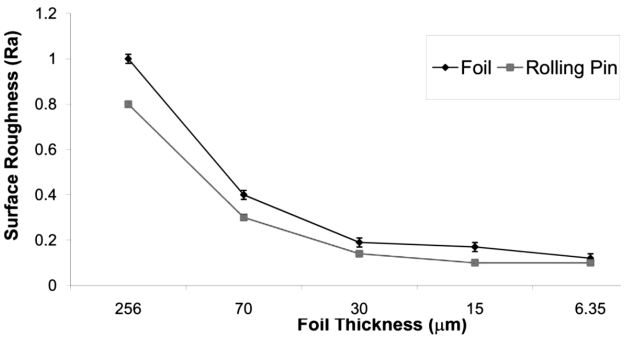

Figure 9: The variation of the surface roughness in foil rolling stages
Slika 9: Spreminjanje hrapavosti površine pri valjanju folij

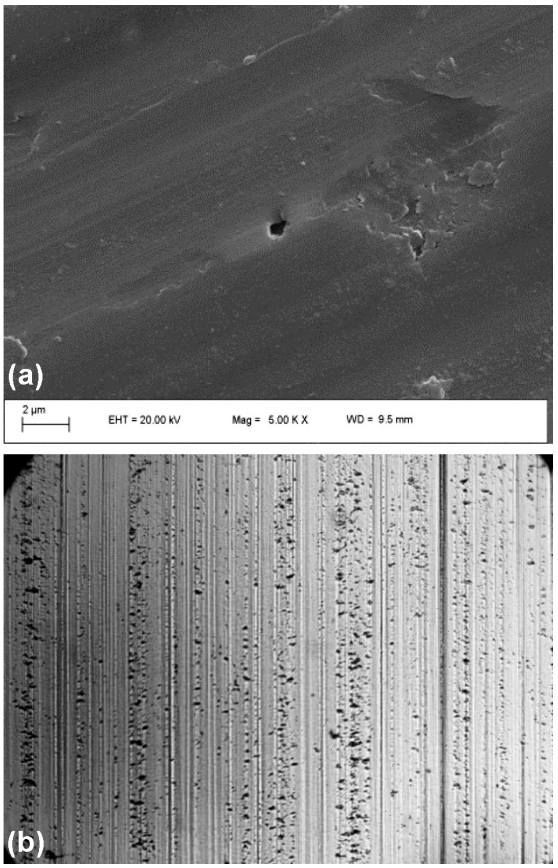

Figure 10: The surface structures: a) SEM image of a pin hole 5000 ×, b) rolling trucks and porous of the surface 200 ×
Slika 10: Struktura površine: a) SEM posnetek luknjice 5000 ×, b) sledi valjanja in poroznost površine 200 ×

stable inter-metallic phases because of high cooling rates, due to kinetic restrictions there is not enough time for the atoms to arrange themselves in a stable structure.

The AFM scanning images indicates that the valley and the peaks are oriented along the rolling direction. The surface roughness of the rolling pin and the foils are very close in almost all cases especially in thinner foils.

Acknowledgements

This work was supported by Necmettin Erbakan University Scientific Research Projects (BAP) Coordinatorships and by the Ministry fo Industry with project No. 01078.STZ.2011-2.

5 REFERENCES

[1] M. Dündar, The Material Properties management on Aluminum sheet production with twin Roll Casting Technique, 13th International Metallurgy and Material Conference, Istanbul, 2006, 1–9

[2] M. S. Salehi, S. Serajzadeh, Simulation of static softening behavior of an aluminum alloy after cold strip rolling, Computational Materials Science, 69 (**2013**), 53–61, doi:10.1016/j.commatsci.2012.11.028

[3] D. Wang, Z. Y. Ma, Z. M. Gao, Effects of severe cold rolling on tensile properties and stress corrosion cracking of 7050 aluminum alloy, Materials Chemistry and Physics, 117 (**2009**), 228–233, doi:10.1016/j.matchemphys.2009.05.048

[4] Z. Liang, C. Junzhou, Y. Shoujie, S. Wenzhou, D. Shenglong, Development of microstructures and texture during cold rolling in AA 7055 aluminum alloy, Materials Science and Engineering A, 504 (**2009**), 55–63, doi:10.1016/j.msea.2008.10.055

[5] S. X. Zhou, Z. Jue, M. Daheng, F. Paul, Experimental study on material properties of hot rolled and continuously hot aluminum strips in cold rolling, Journal of Material Processing Technology, 134 (**2003**), 363–373, doi:10.1016/S0924-0136(02)01121-4

[6] J. G. Lenard, The effect of roll roughness on the rolling parameters during cold rolling of an aluminum alloy, Journal of Materials Processing Technology, 152 (**2004**), 144–153, doi:10.1016/j.jmatprotec.2004.03.026

[7] J. G. Lenard, S. Zhang, A study of friction during the lubricated cold rolling of an aluminum alloy, Journal of Materials Processing Technology, 72 (**1997**), 293–30, doi:10.1016/S0924-0136(97)00183-0

[8] K. S. S. Satheesh, T. Raghu, Structural and mechanical behavior of severe plastically deformed high purity aluminum sheets processed by constrained groove pressing technique, Materials and Design, 57 (**2014**), 114–120, doi:10.1016/j.matdes.2013.12.053

[9] G. Liv, Development of surface topography during aluminum cold rolling of twin-roll cast, Wear, 192 (**1996**), 216–227, doi:10.1016/0043-1648(95)06809-0

[10] B. Felipe, S. M. Elisangela, R. G. Pedro, C. Noe, R. Rudimar, G. Amauri, Laser remelting of Al–1.5 wt% Fe alloy surfaces: Numerical and Experimental analyses, Optics and Lasers in Engineering, 49 (**2011**), 490–497, doi:10.1016/j.optlaseng.2011.01.007

[11] M. S. Debkumar, C. Suryanarayana, F. H. Froes, Structural Evolution in Mechanically Alloyed Al–Fe Powder, Metallurgical and Materials Transactions A, 26 (**1995**) 8, 1939–1946

[12] S. S. Nayak, H. J. Chang, D. H. Kim, S. K. Pabi, B. S. Murty, Formation of metastable phases and nanocomposite structures in rapidly solidified Al–Fe alloys, Materials Science and Engineering A, 528 (**2011**), 5967–5973, doi:10.1016/j.msea.2011.04.028

[13] C. A. Aliravci, M. O. Pekguleryuz, Calculation of phase diagrams for the metastable Al-Fe phases forming in direct-chill (DC)-cast aluminum alloy ingots, Calphad, 22 (**1998**), 147–155, doi:10.1016/S0364-5916(98)00020-0

[14] M. Gremaud, M. Carrard, W. Kurz, The microstructure of rapidly solidified Al-Fe alloys subjected to laser surface treatment, Acta Metallurgica et Materialia, 38 (**1990**) 12, 2587–2599, doi:10.1016/0956-7151(90)90271-H

[15] P. J. Appsa, J. R. Bowenb, P. B. Prangnell, The effect of coarse second-phase particles on the rate of grain refinement during severe deformation processing, Acta Materialia, 51 (**2003**), 2811–2822, doi:10.1016/S1359-6454(03)00086-7

[16] C. M Allen, S. Kumar, L. Carrol, K. A. Q. O'Reilly, H. Cama, Electron beam surface melting of model 1200 Al alloys, Materials Science and Engineering A, 304 (**2001**), 604–607, doi:10.1016/S0921-5093(00)01543-4

[17] M. Aghaie-Khafri, R. Mahmudi, Flow localization and plastic instability during the tensile deformation of Al alloy sheet, JOM, 50 (**1998**), 50–52, doi:10.1007/s11837-998-0287-5

[18] T. Tunçay, D. Özyürek, The effects on microstructure and mechanical properties of filtration in Al-Si-Mg alloys, Journal of the Faculty of Engineering and Architecture of Gazi University, 29 (**2014**), 271–279

[19] A. Benallal, T. Berstad, T. Børvik, O. S. Hopperstad, I. Koutiri, R. Nogueira de Codes, An experimental and numerical investigation of the behavior of AA5083 aluminum alloy in presence of the Portevin–Le Chatelier effect, International Journal of Plasticity, 24 (**2008**), 1916–1945, doi:10.1016/j.ijplas.2008.03.008

[20] J.-M. Lee, S.-B. Kang, T. Sato, H. Tezuka, A. Kamio, Fabrication of Al/Al3Fe composites by plasma synthesis method, Materials Science and Engineering A, 343 (**2003**), 199–209, doi:10.1016/S092-5093(02) 00380-5